



Molecular Dynamics Simulation of Natural Gas Liquefied LNG Boil-Off

Mesli Fouzia^{1,3*}, Missoum Nouredine^{2,3} and Ghalem Saïd^{1,3}

¹Department of Chemistry, Aboubekr Belkaid University of Tlemcen, Algeria

²Hassiba Benbouali University of Chlef, Algeria

³Laboratory of Natural and Bioactive Substances (LASNABIO), Algeria

*Corresponding Author: Mesli Fouzia, Department of Chemistry, Aboubekr Belkaid University of Tlemcen, Algeria.

Received: July 08, 2019; Published: September 27, 2019

DOI: 10.31080/ASMS.2019.03.0423

Abstract

Background: A simulation of natural gas liquefied LNG Boil-Off was carried out using two different thermodynamic cycles with the Lennard Jones potential model. We have calculated the new parameters of the Lennard Jones potential using an iterative algorithm with a mean square method. This adapted model allows us to determine the characteristics for each state point. We applied this model to study the LNG properties through the Brayton cycle and the Carnot cycle by molecular dynamics. Thermodynamic, dynamic and structural properties for both the microcanonical NVT and the isothermal-isobaric NPT ensembles of LNGB and LNGC systems from three state points SP1, SP4 and SP8 were elaborated. Results show a good prediction on transport properties from the calculated values of self-performance coefficient and the compressibility factor for the cycle of Brayton. Results show also that increasing the compression ratio is the most direct way to increase the overall power output of a Brayton system. Our results are in good agreement with theoretical and experimental outcomes.

Keywords: LNG Boil-Off; Brayton Cycle; Carnot Cycle; Thermodynamic Properties

Introduction

Molecular simulation methods techniques are profitably employed nowadays in several industrial sectors. The use of molecular simulation includes, for instance, the design of new molecules or phases through the prediction of their physical or chemical properties. In literature, much potential are proposed. The potential of Kihara [1], Lennard-Jones [2] and Stillinger-Weber [3]. Several researchers have investigated the study of Liquefaction of LNG Boil-Off. In a previous works we studied the site-site interaction of LNG properties [4].

We also studied the different properties of CH₄-N₂ system by MD for the SP1, SP4, and SP8 points [5]. And for binary and ternary mixtures Re-Liquefaction of LNG for the SP1 to SP9 points [6]. Our aim in this work is to confirm the efficiency of two thermodynamics cycles namely Brayton cycle it is also known under the name of Joule cycle and Carnot cycle is a theoretical thermodynamic cycle for a motor ditherme taking in a account the diffusion properties of each cycle.

In the objective to minimize the LNG gas los in to atmosphere. And to compare this theoretical results with experimental outcomes. Experiment shows that, the Brayton cycle present most important efficiency compared to Carnot cycle [7].

Materials and Methods

The system of interest is Re-Liquefaction of LNG Boil-Off Gas state thermodynamics at different points SP_i (ρ , T), summarized in Table 1. Each point is characterized by the density ρ (g cm⁻³) of the system and its temperature T (°C). In this work, the Re-Liquefaction of LNG Boil-Off Gas which are consisted of N (32,864, and 1500) molecules in freely rotating state have been studied.

For these calculations are considered through the spherical models of Lennard-Jones [2].

$$U_{LJ}(r) = 4\epsilon \left[\left(\frac{\sigma}{r} \right)^{12} - \left(\frac{\sigma}{r} \right)^6 \right] \text{ Eq.1}$$

In these calculations, the overall runtime is of 500ps with an equilibration period of 125ps and data production period reaching up to 125 ps. Previously, the Nosé thermostat process is applied, whereas the isothermal-isobaric NPT is incorporated to the Parinello-Raman integration scheme. When the equilibrium is reached, some properties are calculated are represent in table 1.

Results and Discussion

We realized our simulation for the SP1, SP4, and SP8 points taken from the phase diagram using the LJ potential model. Then we have compared the obtained properties to evaluate the efficiency

potential	LJ	g _{ij} /KB (K)	Q*/W Q*/W LNGB LNGC		State point	T (K)	T*	(g/cm ³)	(g/cm ³)	(g/cm ³)	(g/cm ³)
			C ₂ H ₆	C ₂ H ₆				N ₂	CH ₄	CH ₄ - N ₂ LNG	
parameters	Crij (Å)		Brayton	Carnot	SP1	91.0	0.6103	0.6537	0.4495	0.4495	0.2697
C....C	3.35 ^(b)	50.00 ^(b)	.56/2.54 524.690	2.53/4.25	SP2	98.8	0.6692	0.6160	0.4407	0.4407	0.2644
C....C ^(a)	-	-	C1 505.000		SP3	105.4	0.7069	0.6363	0.4331	0.4331	0.2598
C....H	3.08 ^(b)	20.73 ^(b)	56/2.45 123.230	.25/4.51	SP4	108.0	0.7243	0.6334	0.4263	0.4263	0.5557
C....H ^(a)	-	-			SP5	110.9	0.7437	0.6291	0.4253	0.4253	0.2551
H....H	2.81 ^(b)	08.60 ^(b)	4.73/3.45 31.799	5.14/3.56	SP6	116.5	0.7813	0.6224	0.4173	0.4173	0.2503
H....H ^(a)	-	-			SP7	122.1	0.8189	0.6182	0.4091	0.4091	0.2454
N....N	3.31 ^(c)	37.30 ^(c)			SP8	125.0	0.8284	0.6124	0.4005	0.4005	0.2403
C....N	3.33	43.18									
H....N	3.06	17.91									

Work reported by WILLIAMS [14].

Table 1: Potential parameters of site-site interactions for C....C, C....H, H....H, N....H, N....N and C....N.

cycle. Using molecular dynamics, we have studied the evolution of the transport various and thermodynamic properties of the LNG Gas in units NVT and NPT systems using the two cited cycle.

Structural properties

The radial distribution functions $g(r)$ may be computed: [8,9].

$$g(r) = \exp \left[-\frac{u(r)}{kT} \right] y(r) \text{ with}$$

$$y(r) = 1 + \sum_{n=1}^{\infty} \rho^n y_n(r) \text{ Eq.2}$$

Where $y(r)$ is known as the cavity distribution function.

State point	RMAX1	RMAX2	RMIN1
Sp ₁ ,sp ₄ ,sp ₈ ^a	4.100	7.700	5.7005-5.750
Sp ₁ ,sp ₄ ,sp ₈ ^b	4.050	7.750	5.7263-5.632
Sp ₁ ,sp ₄ ,sp ₈ ^c	4.050	7.750	5.750-5.850
Sp ₁ ,sp ₄ ,sp ₈ ^d	1.050	1.750	5.7505-5.850
Sp ₁ ,sp ₄ ,SP ₈ ^e MCR	4.236	7.354	5.456-5.542
Sp ₁ ,sp ₄ ,sp ₈ ^e MCR	4.025	7.556	5.652-5.765
Sp ₁ ,sp ₄ ,sp ₈ ^f LNGB	1.522	5.245	4.250-4.201
Sp ₁ ,sp ₄ ,sp ₈ ^f LNGC	1.452	5.210	4.562-5.025

a: Site-site interaction (Belkacem., *et al.* 2005). b: Spherical approximation (Tchouar., *et al.* 1998). [10]. c: Sesé work (Sesé,1992, 1994). d: Experimental work (Sesé, 1992, 1993, 1994)
e: Mesli., *et al.* f: Present work.

Table 2: Values of maximum and minimum for $g(r)$ C....C. LNGB: (Liquefied Natural gas of Brayton LNGC: Liquefied Natural gas of Carnot).

Our results show

The first Rmax1 for Brayton and Carnot cycle respectively are: = 1.522 Å and Rmax1= 1.452 Å . The second maximum is Rmax2 = 5.245 Å for the LNGB cycle and Rmax2 = 5.210 Å for LNGC cycle. However, the first minimum is Rmin1 = 5.456– 5.542 Å for the three state points of Brayton cycle. The first minimum is Rmin1 = 4.250–4.201 Å for the three state points of Carnot cycle. In Figure 1, the most important orientations responsible for the peaks are represented. Using the ACD/ChemSketch. Our results are in good agreement with results cited by Murad., *et al.* [11] concerning the prediction of discontinuities over time.

Obtained results for SP1 point are presented in figure 1.

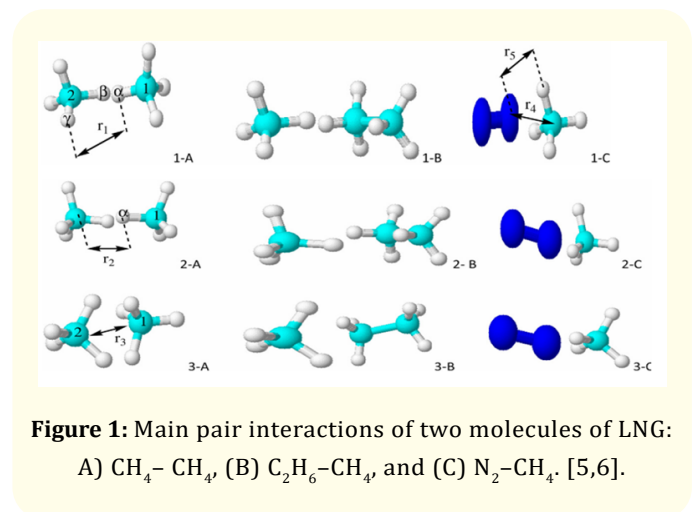


Figure 1: Main pair interactions of two molecules of LNG: A) CH₄-CH₄, B) C₂H₆-CH₄, and C) N₂-CH₄. [5,6].

Thermodynamic properties

Using the MD simulation approach, we have studied the thermodynamic properties evolution of LNG Boil-Off Gas in NVT and NPT ensemble. The internal energy is illustrated by the following form. The average internal energy per particle is [12].

$$\frac{\langle E \rangle}{N} = \frac{3}{2} k_B T + \frac{\langle U_N \rangle}{N} = \frac{3}{2} k_B T + \frac{\rho}{2} \int_V dr u(r) g(r, \rho, T) \text{ Eq.3}$$

Where the number of particle is in the system, ρ is the number density, $u(r)$ is the pair potential In this study, we give the evolution of the internal energy and compressibility factor for the LNG systems results are presented in Figure 2 and Figure 3.

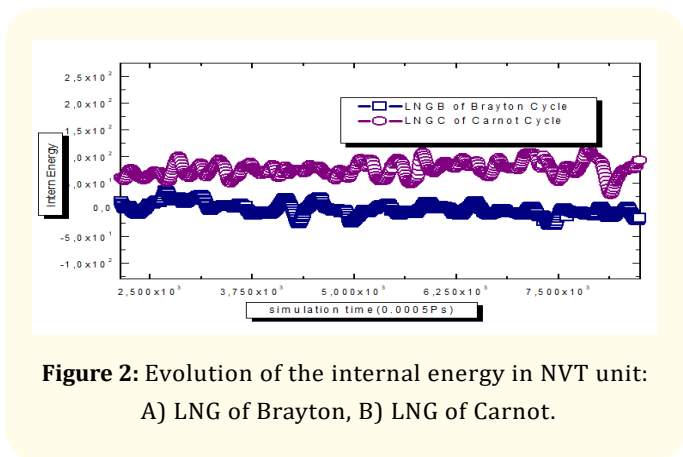


Figure 2: Evolution of the internal energy in NVT unit: A) LNG of Brayton, B) LNG of Carnot.

The factor of compressibility is calculated by Redlich-Kwong-Soave (R-K-S) from the following equation:

$$Z = \frac{PV}{RT} = \frac{V}{(V-b)} - \frac{aV}{RT(V_2 + c_1.b.V + c_2.b_2)} \text{ Eq.4}$$

Where P : absolute Pressure V : Volume molar of the mixture, R : Constant of perfect gases, T : Temperature of the mixture; a/b/c1/c2- Constant calculated for mixtures and Z Factor of compressibility. The pressure of the system can also be calculated by relating the 2nd virial coefficient to $g(r)$. The pressure can be calculated as follows:

$$p = \rho k_B T - \frac{2}{3} \Pi \rho^2 \int_0^\infty dr \frac{du(r)}{dr} r^3 g(r) \text{ Eq.5}$$

Where T is the temperature and k_B is Boltzmann's constant.

And cop is determined for the report of the quantity of heat and the work exerted on the system of refrigeration. The performance coefficient can be calculated as follows:

$$COP = \frac{|Q|}{W} \text{ Eq.6}$$

Where Q is the useful heat for the exchanger and W is absorptive mechanical work by the compressor. For refrigerant system, the pressure and cop are stabilized in time (Figure 3,4).

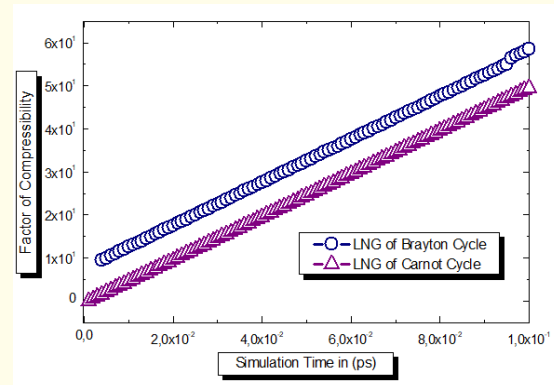


Figure 3: Evolution of Factor of compressibility in NVT unit : A) LNG of Brayton, B) LNG of Carnot.

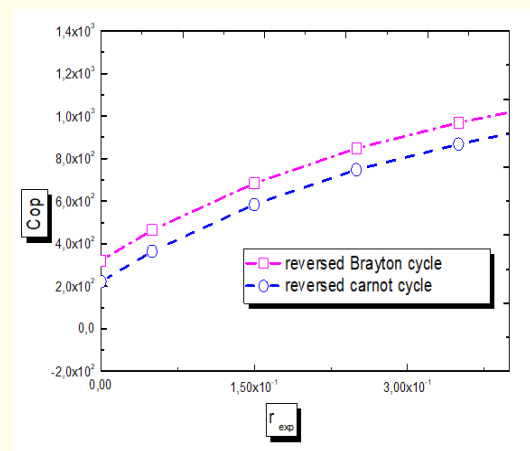


Figure 4: The effect of rejection and refrigeration temperature effectiveness on COP in NVT unit: A) LNG of Brayton, B) LNG of Carnot.

Calculations were achieved near the triple point 91K. The thermodynamic properties (P^* , Z^* , U^* , E^*) are calculated in reduced units [13,14]. All our results are given in table 3.a.b.

Table 3 a and b show that for the two models, the compressibility factor decreases by increasing the temperature and the performance coefficient increases then the system will be less viscous. Therefore, self- performance coefficient and factor of compressibility vary in irregularly style at the SP1 and SP4 points in the LJ model. We note that the increasing of the particles number does not affect the system properties mainly for the COP and the Z (table 3a). However, the situation is reversed when the composition of the system varied. Indeed, at high composition of the LNGB Brayton cycle (XLNG = 90/10%), the COP is the highest for the smallest factor of Z value; (table 3b). We note that the resultats is opposite for LNGC cycle of Carnot. Therefore the cycle of Brayton describes correctly the studied LNG system for any point of the phase diagram and perfectly stabilizes the system.

State point	Method	N	P*	U*	Z*	COP*	E*
SP1	NVT LNGB	32	1.181 ± 0.500	-2.505 ± 0.04	5.015 ± 0.050	0.165 ± 0.005	-3.31 ± 0.03
	NPT LNGB		1.452 ± 0.501	-3.120 ± 0.04	4.014 ± 0.010	0.152 ± 0.002	-3.33 ± 0.05
			2.542 ± 0.202	-2.504 ± 0.05	3.524 ± 0.044	0.452 ± 0.002	-2.34 ± 0.03
			1.543 ± 0.302	-3.525 ± 0.05	5.504 ± 0.020	0.3458 ± 0.00	-2.31 ± 0.03
	NVT LNGB	865	1.050 ± 0.531	-2.305 ± 0.042	5.012 ± 0.040	0.152 ± 0.005	-3.12 ± 0.030
	NPT LNGB		1.426 ± 0.521	-4.10.0.105	4.013 ± 0.010	0.165 ± 0.004	-5.5 ± 0.0205
			2.355 ± 2.556	-2.253 ± 0.042	5.505 ± 0.024	0.455 ± 0.005	-5.15 ± 0.040
			2.545 ± 1.525	-4.054 ± 0.024	6.504 ± 0.040	0.352 ± 0.005	-5.12 ± 0.030
	NVT LNGB	1500	1.050 ± 0.232	-3.300 ± 0.045	5.072 ± 0.050	0.156 ± 0.005	-3.30 ± 0.031
	NPT LNGB		1.554 ± 0.231	-5.125 ± 0.042	6.015 ± 0.010	0.155 ± 0.005	-3.55 ± 0.021
			2.555 ± 2.422	-4.255 ± 0.054	5.505 ± 0.024	0.545 ± 0.004	-2.53 ± 0.041
			1.225 ± 1.224	2.3222 ± 0.02	4.520 ± 0.050	0.355 ± 0.004	-2.70 ± 0.010
SP4	NVT LNGB	32	0.4052 ± 0.82	-2.015 ± 0.045	5.512 ± 0.045	0.252 ± 0.025	-2.22 ± 0.032
	NPT LNGB		0.425 ± 0.855	-5.204 ± 0.005	6.056 ± 0.052	0.252 ± 0.034	-3.20 ± 0.013
	NVT LNGC		0.525 ± 2.525	-4.545 ± 0.052	6.560 ± 0.052	0.352 ± 0.065	-3.74 ± 0.042
	NPT LNGC		0.251 ± 5.725	-4.503 ± 0.040	6.425 ± 0.040	0.3570 ± 0.0	-2.70 ± 0.020
	NVT LNGB	865	0.0201 ± 0.55	-3.015 ± 0.070	5.015 ± 0.040	0.225 ± 0.025	-4.23 ± 0.022
	NPT LNGB		0.121 ± 0.252	-3.275 ± 0.070	5.030 ± 0.020	0.225 ± 0.032	-3.23 ± 0.55
	NVT LNGC		0.124 ± 2.521	-3.545 ± 0.080	7.522 ± 0.040	0.321 ± 0.065	-3.25 ± 0.041
	NPT LNGC		0.2212 ± .3.24	-3.573 ± 0.050	7.50 1 ± 0.07	0.3274 ± 0.04	-5.73 ± 0.010
	NVT LNGB	1500	0.0003 ± 0.85	-3.09 ± 0.053	6.079 ± 0.005	0.232 ± 0.025	-2.73 ± 0.032
	NPT LNGB		1.124 ± 0.858	-4.27 ± 0.060	6.037 ± 0.028	0.220 ± 0.004	-4.73 ± 0.013
	NVT LNGC		0.420 ± 2.526	-4.46 ± 0.053	6.642 ± 0.072	0.325 ± 0.024	-3.70 ± 0.043
	NPT LNGC		2.241 ± 3.741	-4.2500.05	6.4056 ± 0.91	0.322 ± 0.0 10	-5.39 ± 0.030
SP8	NVT LNGB	32	0.401 ± 0.44	-3.0221 ± 0.05	5.05 ± 0.0722	0.452 ± 0.202	-1.20 ± 0.021
	NPT LNGB		0.514 ± 3.154	-2.0245 ± 0.06	6.005 ± 0.051	0.315 ± 0.215	-3.56 ± 0.022
	NVT LNGC		0.361 ± 0.545	-5.03 ± 0.0521	6.454 ± 0.064	0.335 ± 0.003	-4.24 ± 0.042
	NPT LNGC		0.310 ± 1.421	-6.040 ± 0.060	5.216 ± 0.042	0.486 ± 0.006	-5.44 ± 0.030
	NVT LNGB	865	0.102 ± 0.842	-4.0211 ± 0.05	5.025 ± 0.052	0.455 ± 0.201	-3.32 ± 0.032
	NPT LNGB		0.111 ± 3.188	-4.6049 ± 0.40	4.005 ± 0.061	0.361 ± 0.2 05	-3.53 ± 0.022
	NVT LNGC		0.161 ± 0.241	-5.05 1 ± 0.021	3.450 ± 0.060	0.350 ± 0.052	-4.33 ± 0.001
	NPT LNGC		0.101 ± 3.411	-6.01 ± 0.0205	7.203 ± 0.045	0.470 ± 0.005	-5.30 ± 0.030

Table 3a: Thermodynamic properties calculated in reduced units. Pressure $P^* = P \sigma^3 / \epsilon$, Energy of configuration $U^* = U / N\epsilon$, LNGB: liquefied natural gas of Brayton.LNGC: liquefied natural gas of Carnot.

Conclusions

In this work, we have studied many properties for LNGB and LNGC mixtures by molecular dynamics. We have calculated the thermodynamic, transport and structural properties for both the NVT and NPT ensembles of Brayton and Carnot cycles from the three points SP1, SP4 and SP8. Then, we have compared the re-

sults between Brayton and Carnot cycles. We have obtained a good prediction on transport properties for performance coefficient and the factor of compressibility of liquefied natural gas according to the cycle of Brayton This last for the refrigeration it uses the turbo expander which edge more efficiently generate refrigeration especially to cryogenic. The situation for Carnot cycle is reversed.

State point	Method	N X LNG (%)	P*	U*	Z*	COP*	E*
SP1	NVT LNGB	90	1.051 ± 0.536	-2.354 ± 0.040	5.012 ± 0.050	0.164 ± 0.006	-4.11 ± 0.015
	NPT LNGB		0.555 ± 0.531	-3.150 ± 0.050	5.017 ± 0.015	0.142 ± 0.005	-5.13 ± 0.021
			1.355 ± 2.556	-3.504 ± 0.050	6.042 ± 0.050	0.452 ± 0.004	-4.14 ± 0.013
			0.254 ± 1.556	-4.205 ± 0.050	5.504 ± 0.050	0.336 ± 0.004	-5.11 ± 0.130
	NVT LNGB	75	0.040 ± 0.934	-3.355 ± 0.052	4.042 ± 0.020	0.152 ± 0.002	-5.22 ± 0.035
	NPT LNGB		1.456 ± 0.934	-5.173 ± 0.052	5.014 ± 0.012	0.155 ± 0.001	-4.54 ± 0.022
			0.355 ± 2.456	-4.554 ± 0.024	5.545 ± 0.025	0.455 ± 0.006	-5.25 ± 0.023
			1.265 ± 1.254	-3.604 ± 0.020	6.525 ± 0.050	0.542 ± 0.004	-5.22 ± 0.032
	NVT LNGB	30	0.060 ± 0.531	-4.350 ± 0.045	5.052 ± 0.050	0.166 ± 0.002	-5.30 ± 0.035
	NPT LNGB		0.464 ± 0.934	-5.144 ± 0.050	6.015 ± 0.015	0.165 ± 0.004	-6.52 ± 0.025
			0.344 ± 2.454	-4.543 ± 0.054	6.545 ± 0.050	0.440 ± 0.002	-4.33 ± 0.033
			0.244 ± 1.244	-6.5422 ± 0.45	4.550 ± 0.030	0.3406 ± 0.005	-5.70 ± 0.030
SP4	NVT LNGB	90	0.0502 ± 0.55	-5.015 ± 0.045	4.015 ± 0.025	0.242 ± 0.024	-4.72 ± 0.022
	NPT LNGB		0.121 ± 0.252	-6.274 ± 0.042	5.034 ± 0.025	0.242 ± 0.030	-1.20 ± 0.012
	NVT LNGC		0.225 ± 2.122	-6.545 ± 0.064	4.553 ± 0.052	0.457 ± 0.062	-5.24 ± 0.022
	NPT LNGC		0.202 ± 23.24	-6.543 ± 0.050	5.426 ± 0.010	0.570 ± 0.011	-6.70 ± 0.032
	NVT LNGB	75	0.021 ± 0.252	-5.717 ± 0.043	6.015 ± 0.025	0.535 ± 0.024	-4.34 ± 0.023
	NPT LNGB		1.23 ± 0.3532	-5.265 ± 0.050	5.034 ± 0.062	0.255 ± 0.035	-5.72 ± 0.213
	NVT LNGC		0.34 ± 2.5220	-6.645 ± 0.040	5.552 ± 0.062	0.351 ± 0.062	-5.76 ± 0.043
	NPT LNGCd		0.218 ± 3.241	-5.573 ± 0.022	4.021 ± 0.51	0.304 ± 0.014	-5.32 ± 0.030
	NVT LNGB	30	0.023 ± 0.851	-5.04 ± 0.0323	5.013 ± 0.025	0.230 ± 0.025	-4.30 ± 0.022
	NPT LNGB		1.124 ± 0.821	-6.05 ± 0.063	6.033 ± 0.022	0.520 ± 0.035	-5.28 ± 0.013
	NVT LNGC		120 ± 2.5220	-6.045 ± 0.073	4.532 ± 0.052	0.505 ± 0.064	-5.20 ± 0.022
	NPT LNGC		0.21 ± 3.2411	-4.230 ± 0.060	5.4213 ± 0.51	0.304 ± 0.014	-5.72 ± 0.032
SP8	NVT LNGB	90	0.3211 ± 0.84	-2.0721 ± 0.055	5.024 ± 0.052	0.502 ± 0.230	-3.20 ± 0.035
	NPT LNGB		0.034 ± 3.188	-5.0241 ± 0.041	7.005 ± 0.050	0.212 ± 0.211	-2 ± 0.59.022
	NVT LNGC		0.363 ± 0.221	-4.273 ± 0.0555	6.465 ± 0.054	0.335 ± 0.064	-4.2 ± 0.042
	NPT LNGC		0.330 ± 3.451	-6.544 ± 0.0600	7.254 ± 0.052	0.206 ± 0.002	-2.5 ± 0.030
	NVT LNGB	75	2.122 ± 0.842	-2.0711 ± 0.055	5.020 ± 0.042	0.405 ± 0.230	-3.22 ± 0.025
	NPT LNGB		0.214 ± 3.122	-3.6649 ± 0.005	5.001 ± 0.005	0.301 ± 0.212	-5.42 ± 0.022
	NVT LNGC		2.362 ± 0.242	-5.831 ± 0.0601	5.450 ± 0.050	0.300 ± 0.022	-4.23 ± 0.041
	NPT LNGC		0.321 ± 3.421	-6.801 ± 0.0605	5.203 ± 0.022	0.400 ± 0.006	-5.48 ± 0.030

Table 3b : Thermodynamic properties calculated in reduced units. Pressure $P^* = P \sigma^{-3}/\epsilon$, Energy of configuration

$U^* = U/N\epsilon$, LNGB: liquefied natural gas of Brayton. LNGC: liquefied natural gas of Carnot.

The diffusion of LNG of Brayton in the liquid is much better than in the LNGC of Carnot. However, the diffusion situation is reversed. From the calculated values of self- performance coefficient and the compressibility factor. Our results confirmed that LNG mixture is in liquid state. We conclude that our simulation model approach very well the experimental data. Our work presents the possibility to determine with a high precision the thermodynamic, dynamics,

and structural properties of LNG for any cycle while basing itself on adequate approximation and to propose a good optimization of the liquefaction process. We hope that this model could be an effectively starting material to study the properties of other complex systems in order to predict the transport phenomenon in the multi-component refrigerants MCR.

Acknowledgements

The authors thank the National Agency for the Development of University Research (ANDRU) in Algeria for its financial support.

Conflict of Interest

The authors declare no conflict interest.

Bibliography

1. T Kihara. "Combination rules for intermolecular potential parameters. I. Rules based on approximations for the long-range dispersion energy". *Advances in Chemical Physics* 5 (1963): 147.
2. JE Lennard-Jones. "On the determination of molecular fields". *Proceedings of the Royal Society A* 106 (1924): 463-477.
3. M Shadman, *et al.* "Ab initio interaction potential of methane and nitrogen". *Physics Letter* 467 (2009): 237-242.
4. F Belkacem and A Krallafa. "Thermodynamic, Structural and Transport of Liquid Methane. An extensive Molecular Dynamics". *The Journal of Chemical Physics* (2005): 15.
5. F Mesli, *et al.* "Thermodynamic, dynamic and structural properties of methane-nitrogen mixture. A molecular dynamics simulation study". *Physical and Chemical News* 56 (2010): 117-127.
6. F Mesli, *et al.* "Molecular dynamics comparative study of methane-nitrogen and methane-nitrogen-ethane system". *Arabian Journal of Chemistry* 4 (2011): 211-122.
7. J H Baek and HM Chang. "Cycle Analysis of 2-Stage Expansion Claude Refrigerator with Turboexpanders". *Journal of Sarek* 6.2 (1994): 130-139.
8. WB Streett and KE Gubbins. "Liquids of Linear Molecules: Computer Simulation and Theory". *Annual Review of Physical Chemistry* 28 (1977): 373-410.
9. L J Lowden and D Chasndler. "A Festschrift from theoretical chemistry Accounts". *The Journal of Chemical Physics* 61(1974): 5228-5241.
10. N Tchouar, *et al.* "Thermodynamic, Structural and Transport Properties of Lennard-Jones Liquid Systems. A Molecular Dynamics Simulations of Liquid Helium, Neon, Methane and Nitrogen". *International Journal of Molecular Sciences* 4 (2003): 595-606.
11. Murad DJ, *et al.* "A thermodynamics for a system under shear". *Molecular Physics* 37 (1979): 725.
12. DJ Evens, *et al.* "Flows Far From Equilibrium Via Molecular Dynamics". *Annual Review of Fluid Mechanics* 18 (1986): 243.

13. MP Allen and DJ Tildesley. "Computer Simulation of Liquids". Clarendon Press, Oxford (1987).
14. Williams DE. "Nonbonded Potential Parameters Derived from Crystalline Hydrocarbons". *The Journal of Chemical Physics* 47 (1967): 4680-4684.

Volume 3 Issue 10 October 2019

© All rights are reserved by Mesli Fouzia, *et al.*